NIH Public Access
Author Manuscript
Nat Chem. Author manuscript; available in PMC 2011 April 1.

Published in final edited form as:
Nat Chem. 2010 October ; 2(10): 847–852. doi:10.1038/nchem.751.

Kinetic resolution of constitutional isomers controlled by selective protection inside a supramolecular nanocapsule

Simin Liu, **Haiying Gan**, **Andrew T. Hermann**, **Steven W. Rick**, and **Bruce C. Gibb***
Department of Chemistry, University of New Orleans, New Orleans, Louisiana 70148, USA

Abstract

The concept of self-assembling container molecules as yocto-litre reaction flasks is gaining prominence. However, the idea of using such containers as a means of protection is not well developed. Here, we illustrate this idea in the context of kinetic resolutions. Specifically, we report on the use of a water-soluble, deep-cavity cavitand to bring about kinetic resolutions within pairs of esters that otherwise cannot be resolved because they react at very similar rates. Resolution occurs because the presence of the cavitand leads to a competitive binding equilibrium in which the stronger binder primarily resides inside the host and the weaker binding ester primarily resides in the bulk hydrolytic medium. For the two families of ester examined, the observed kinetic resolutions were highest within the optimally fitting smaller esters.

The simple act of compartmentalization is essential to chemistry. To an organic chemist, a round-bottomed flask is both a means of promoting a reaction by keeping reagents in, and stopping reactions by keeping species such as adventitious water out. In parallel with these concepts, in recent years supramolecular chemists have developed the idea of using container molecules as yocto-litre flasks to promote new reactions[1–23]. However, there has been little progress in using container molecules as a means of protection. Indeed, to our knowledge, there has been only one reported example of supramolecular protection, where a primary amine product was prevented from over-alkylation by complexation to a cavitand[24].

While considering the idea of protection via compartmentalization, it occurred to us that one of the strengths of container molecules that fully envelop their guests is their ability to recognize subtle differences between the gross overall forms of molecules. Consequently, many of the container molecules in the literature could theoretically bring about not just the familiar kinetic resolution of stereoisomers[25–28], but also the as yet unexplored topic of the kinetic resolution of constitutional isomers. Regarding the latter, there are of course many examples of compounds only being available as mixtures with constitutional isomers or constitutionally similar molecules. Hence, establishing a proof-of-principle that container molecules could effect such purifications could be quite powerful. In this Article, we report on the ability of supra-molecular nanocapsules to bring about the kinetic resolution of constitutionally isomeric long-chain esters. More specifically, we show that the capsule formed by water-soluble host

*Correspondence and requests for materials should be addressed to B.C.G. bgibb@uno.edu.

Author contributions
B.C.G. and S.L. conceived and designed the experiments. S.L. synthesized esters **2**–**6** and performed the experiments involving these guests. H.G. and A.T.H contributed equally to the syntheses and experiments involving esters **7**–**11**. B.C.G. wrote the paper.

Additional information
The authors declare no competing financial interests. Supplementary information and chemical compound information accompany this paper at www.nature.com/naturechemistry. Reprints and permission information is available online at http://npg.nature.com/reprintsandpermissions/.

NIH-PA Author Manuscript
NIH-PA Author Manuscript
NIH-PA Author Manuscript

NIH-PA Author Manuscript

NIH-PA Author Manuscript

NIH-PA Author Manuscript

1 can protect encapsulated esters from reaction occurring in bulk solution, and that the degree of protection is intimately tied to the goodness-of-fit between capsule and guest.

The supramolecular capsules central to this investigation were assembled by the dimerization of water-soluble, deep-cavity cavitand **1** (Fig. 1)[29–31]. This host is a bowl-shaped amphiphile composed of a concave hydrophobic pocket, a wide hydrophobic rim, and a convex outer surface 'coated' with eight water-solubilizing carboxylic acid groups. Because of these structural features, in aqueous solution the host is essentially monomeric, but the presence of a suitable guest molecule triggers dimerization of the host and encapsulation of the guest (or guests). Driven by the hydrophobic effect, this assembly occurs for molecules as small as propane[32], as large as steroids[33] and as polar as triethylene glycol derivatives[34].

As a proof-of-principle that container molecules can lead to the kinetic resolution of constitutional isomers, we examined how the presence of capsule $\mathbf{1}_2$ affected the hydrolysis of two families of esters in aqueous 18 mM NaOH. The first series of constitutionally isomeric esters (**2**–**6**; volume, ~228 Å^3; Fig. 1) was selected on the basis that they would optimally fill the inner space of the capsule. We have previously shown that for *n*-alkanes, dodecane and tridecane have the optimal volume for filling capsule $\mathbf{1}_2$; they are neither so small that there is too much empty space within the capsular complex, nor too big such that guest mobility is overly restricted[35]. With this information we viewed methyl decanoate **2**, ethyl nonanoate **3**, propyl octanoate **4**, butyl heptanoate **5** and pentyl hexanoate **6** as ideal constitutionally isomeric guests for the capsule (Fig. 1). The second set of five (16 non-hydrogen atom) esters was chosen because they were anticipated to nearly fill the inner space of the capsule (volume, ~283 Å^3). These were methyl tridecanoate **7**, ethyl dodecanoate **8**, butyl decanoate **9**, hexyl octanoate **10** and heptyl heptanoate **11** (Fig. 1).

As expected, the calculated physical properties of esters **2**–**6** are very similar (Table 1). Using ^{1}H NMR (nuclear magnetic resonance) spectroscopy, we individually examined the hydrolysis of each of the free esters **2**–**6** (see Supplementary Information). As they had limited solubility in pure water, we determined the rate constants for each ester (0.8 mM) in 3:7 acetone-d_6:D_2O containing 10 mM NaOH (T = 26 °C). The excess of base ensured that the reaction, following a $B_{AC}2$ mechanism, was pseudo-first order in ester. As anticipated, there was little difference between the hydrolysis rates of the free esters (Table 1). At 26 °C, the slowest hydrolysis rate was observed for pentyl and hexyl esters **5** and **6**, and the fastest rate for methyl ester **2**. However, the fastest rate of hydrolysis was only ~3 times faster than the slowest rate, an insufficiently large difference for a useful kinetic resolution.

^{1}H NMR was subsequently used to confirm that esters **2**–**6** formed 2:1 host–guest complexes with host **1**. Figure 2 shows the ^{1}H NMR spectrum of such a complex with ester **6**. A combination of peak shift data and information from correlation spectroscopy (COSY) experiments (see Supplementary Information) confirmed that this guest, and indeed all the guests discussed here, bound with each methyl group anchored deeply into a tapering pole of the capsule. As a result of the tapering topology of the polar regions of the cavity, signals from groups residing therein are shifted considerably more than those located at the equatorial region of the capsule. In this particular case, the two methyl groups denoted C1 and C10 (see Fig. 2) were shifted (δΔ) upfield by 3.76 and 3.71 ppm, respectively, to appear at approximately −3 ppm. In contrast, the methylenes of C5 and C6 were shifted by only −1.71 and −1.62 ppm, respectively. In such a pole-to-pole orientation, the guests are slightly too long to adopt a fully extended conformation, but we observed no evidence from nuclear Overhauser effect spectroscopy (NOESY) NMR that any of the guests adopted well-defined helical structures to allow them to efficiently pack the cavity[35,36].

NIH-PA Author Manuscript

NIH-PA Author Manuscript

NIH-PA Author Manuscript

Having confirmed that each guest forms a 2:1 host–guest complex, a network of cross-checking competition experiments (see Supplementary Information) was performed to determine the relative binding constants for the five guests. Figure 2 (inset) shows one example of guest competition, and the complete K_{rel} series is presented in Table 1. The weakest binding guest proved to be propyl ester **4**, with increasing association constants noted for the series **3** < **5** < **6**, <**2**. Considering the pole-to-pole binding of the guests, we view this binding affinity series to be guided by two principle factors. First, 'moving' the ester group from the centre of the long chain towards the terminus results in increased steric clash between host and guest, because with the methyl of the alkoxy group anchored into a pole, the considerably broader ester group (relative to the main chain) must be accommodated in progressively narrower sections of the binding cavity. Hence, binding decreases for the series **6** > **5** >**4**. Counteracting this steric clash, however, are ever-present attractive $–CH_3…\pi$ interactions, which increase significantly as the electronegative alkoxy oxygen is positioned close to the terminus and the C–H bonds of the methyl group undergo increased polarization. This leads to a slight increase in the relative binding constant of **3** versus **4**, and a two orders of magnitude increase in the strength of binding of **2** over **3**.

We subsequently turned to the second set of esters (**7**–**11**), those that were envisioned to essentially fill the cavity of the capsule (Fig. 1). As anticipated, these guests also formed strong 2:1 host–guest complexes (see Supplementary Information), and a similar network of cross-checking competition experiments revealed that the relative binding affinities (K_{rel}) for **7**–**11** were 93.7, 1.4, 1.0, 6.3 and 5.7. Thus, for this series of guests, binding affinity increases for **9** < **8** < **11** <**10** < **7**. This series parallels that of the 13 non-hydrogen atom series; that is, it is energetically preferable for the guest to have a central ester group that can be located at the equatorial region of the cavity, but binding of the methyl ester is enhanced over the other esters because the polarized C–H bonds lead to strong $CH_3 \cdots \pi$ interactions. However, the range of binding affinities of the larger guests is only half that of the first series, presumably because steric repulsion is playing a larger role in the stability of the complexes in which the ester group is located in a tapering polar region.

With relative binding constants established, competitive hydrolysis experiments were then performed using 1:1 mixtures of all the possible combinations of esters **2**–**6**. For each experiment, the concentrations of each species in D_2O were as follows: capsule $\mathbf{1}_2$ (0.5 mM), ester 'a' (0.5 mM), ester 'b' (0.5 mM) and NaOH (18 mM). This ensured that there were 10 equiv. of base after deprotonation of the cavitand, and enough capsule to bind exactly half of the ester mixture. A preliminary experiment with a single ester as guest revealed <5% reaction at room temperature after 1 month. Consequently, all experiments were carried out at 100 °C, with each reaction monitored by ^{1}H NMR to determine the point at which the fastest hydrolysing ester had undergone complete reaction. Integration of signals from the host (1:1 host–product complex and 2:1 capsule–ester complex) directly gave the percentage hydrolysis of the slower reacting isomer, which was itself identified by inspection of the bound guest region. However, if desired, the remaining ester could simply be isolated from the other materials by extraction into chloroform. The results from these resolutions are summarized in Table 2.

The data in Table 2 illustrate that, because the hydrolysis rates of the free esters are so similar (both at room temperature and the calculated rates at 100 °C, *vide infra*), a rule-of-thumb is apparent within this series of esters. If pairs of esters have similar K_{rel} values, for example, **3** versus **4** and **5** versus **6**, then no kinetic resolution is observed. In contrast, if the K_{rel} values differ by approximately one order of magnitude, then fair kinetic resolutions are observed (for example, **2** versus **5**, **2** versus **6**, **3** versus **5**, **3** versus **6**, **4** versus **5** and **4** versus **6**). Finally, if the K_{rel} values differ by two orders of magnitude then good kinetic resolutions are observed

NIH-PA Author Manuscript

NIH-PA Author Manuscript

NIH-PA Author Manuscript

(**2** versus **3** and **2** versus **4**). The best outcome was observed between **2** and **4**; in this case, when all of **4** had reacted, 84% of **2** still remained.

We also examined competition experiments for the second set of esters; however, for this series resolution was much lower. Thus, in a competition between the best (**7**) and worst (**9**) guests, the kinetic resolution noted was only 19%. Complete consumption of **9** also resulted in 81% of **7** undergoing hydrolysis. The reasons for these inferior resolutions are potentially complex (*vide infra*), but one factor may be the relatively weak binding constants of the second series of esters (**7**–**11**). Thus, by means of competition experiments and calculation, the following decreasing order of binding affinities (K_{rel}) was noted for the combined series of esters: **2** (1,350.0), **6** (140.3), **7** (93.7), **5** (88.2), **3** (14.0), **4** (8.4), **10** (6.3), **11** (5.7), **8** (1.4), **9** (1). It is clear that the range of affinities within the first series of esters is much larger than in the second (ratio of K_{rel} values for **2:4** and **7:9** are 161 and 94, respectively). In addition, the second series binds much more weakly; the best guest (**7**) binds with approximately the same affinity as mid-ranged guest **5** from the first series. In other words, four of the five guests from the second series (**8**–**11**) bind more weakly than the weakest binder of the first (**4**). Both these factors can be expected to diminish the kinetic resolution.

In addition to determining resolutions within each family of esters, we also examined the resolution of the two methyl esters **2** and **7**. The K_{rel} values for these two esters were calculated to be 14.4 and 1, respectively, and experimentally determined to be 18 and 1. Based on the results from Table 2, resolution of these two guests would be ~50% in favour of **2**. However, the resolution was observed to be only 15%. The relatively poor resolutions obtained for guests **2** and **7** as well as **7** and **9**, compared to those obtained within the first series of esters **2**–**6**, suggest that the aforementioned rule-of-thumb may only be appropriate within specific series of guests. To better explain the results, we sought information about the mechanism by which these resolutions arise by examining the hydrolysis of each individual ester as a 2:1 complex with the host. A comparison between the kinetic traces for the hydrolysis of ester **6** in the absence (26 °C, 3:7 acetone-d_6:D_2O, excess NaOH) and in the presence (100 °C, D_2O, excess NaOH) of the capsule is shown in Fig. 3. Even though the latter was carried out at a much higher temperature, hydrolysis was much slower. This suggests that the rate-determining step in the hydrolysis of the free ester, that is, hydroxide attack of the carboxyl carbon, is not the rate-determining step in the encapsulation reactions. Instead this is likely to be the opening of the capsule. Supporting this notion is the effect of adding a good (inert) guest to these hydrolysis processes. Thus, a pair of identical experiments monitoring the hydrolysis of encapsulated **4** showed the expected slow hydrolysis until one reaction was spiked by the addition of excess dodecane. The addition of this good guest led to the ejection of the ester and its complete hydrolysis within 10 min (see Supplementary Information).

In Fig. 3 it can be seen that the two curves are obviously very different. The kinetic trace for the host-free solution fits a simple pseudo-first order reaction, but this is not the case in the presence of the host. With the rate-determining step being the opening of the capsule, there are two possible mechanisms to explain the change in kinetics. Either the ester guest leaves the capsule and is hydrolysed in bulk solution, or hydroxide enters the capsule and brings about hydrolysis of the bound ester. Our previous studies have revealed that the interior of the capsule is essentially dry when it is occupied by a reporting guest[3], and consequently our assumption is that the ester must leave the capsule to react.

Assuming this to be the case, the observed hydrolysis can be expected to fit the kinetic scheme defined by equations (1) to (3).

NIH-PA Author Manuscript

NIH-PA Author Manuscript

NIH-PA Author Manuscript

$$H_2G_{ester} \underset{k_{-1}}{\overset{k_1}{\rightleftharpoons}} H_2 + G_{ester} \xrightarrow[Base]{k_2} P_{carboxylate} + P_{alcohol} \quad (1)$$

$$\frac{d[P_{carboxylate}]}{dt} = k_2[G_{ester}][Base] = k_{obs}[G] \quad (2)$$

$$\frac{d[G_{ester}]}{dt} = k_1[H_2G_{ester}] - k_{-1}[G_{ester}][H_2] - k_2[G_{ester}][Base] \quad (3)$$

In this scheme, k_1 corresponds to the rate of dissociation of the ester from the capsule, k_{-1} is the corresponding rate of association, k_2 is the rate constant for reaction of the free ester, and k_{obs} is the observed rate constant for reaction of the free ester. In all cases these values are for systems at 100 °C. Unfortunately, a combination of an overly fast reaction and peak broadening prevented the use of ^{1}H NMR to directly measure k_{obs} at 100 °C. Therefore, to calculate k_{obs} for each ester we determined their rate constants of hydrolysis at seven different temperatures (16–30 °C) and used these data to construct Arrhenius plots (see Supplementary Information). Table 3 lists the obtained activation energies, pre-exponential factors, estimated rate constant at 100 °C, and the errors associated with each of these parameters. As can be seen from the table, errors in the calculated rate constants at 100 °C were good (4.3–7.0%); however, there was no significant difference in the rate constants for the hydrolysis of esters **5** and **6**.

Focusing on esters **2**, **3**, **4** and **6**, we next examined how well these data fitted the kinetic scheme defined by equation (1). More specifically, using the calculated k_2 values we numerically solved the coupled differential equations (2) and (3) using a first-order Euler method (see Supplementary Information) to determine the values of k_1 and k_{-1} that led to the best fit of the experimental data (Fig. 4). The resulting predicted association constants at 100 °C ($K_{a(100)} = k_1/k_{-1}$) were 5.1×10^6 M^{-1} (**2**), 1.2×10^4 M^{-1} (**3**), 1.7×10^4 M^{-1} (**4**) and 2.9×10^4 M^{-1} (**6**). Compounding errors prohibit us from interpreting too much from these values, but it should be noted that these data parallel the experimental data obtained at room temperature: that is, $K_{a(100)}$ **2** > **6** > **3** ≈ **4**.

The fits obtained from these analyses varied from reasonable to very good (χ^2/number of points = 9.25, 11.3, 4.16 and 2.72 for esters **2**, **3**, **4** and **6**, respectively). It is unclear why there are more modest fits for **2** and **3**; however, two 'first thoughts' do not survive scrutiny. First, if the products of hydrolysis—either the carboxylate or the alcohol—were in competition with the ester for the capsule, the fit would be good early in the reaction but deviate at later stages, when greater competition from the products would lead to the actual rates being faster than predicted. However, the reverse is true for esters **2** and **3**; the actual rates are faster at the early stages (particularly in the case of **2**), and slower nearer the end of reaction (for both **2** and **3**). Furthermore, we determined that the best guest of all the products formed from esters **2**–**6**, that is, the decanoate ion, bound with a K_{rel} value of 1/40,000 of ester **2**. For these reactions, the gulf between the association constants of the starting materials and products is therefore too large for product binding to play a major role. It is also unlikely that the modest fit of **2** and **3** arises because hydroxide can enter the capsule. Assuming that the kinetic stability of the different ester complexes parallels their observed thermodynamic stability, it would be esters **3**, **4** and **6** that would be expected to have modest fits. In addition, we have previously observed highly regio-selective reaction when singlet oxygen enters the capsule and reacts with a specifically oriented bound guest[30], in which case it is the most accessible hydrogen atom that

NIH-PA Author Manuscript

NIH-PA Author Manuscript

NIH-PA Author Manuscript

is extracted. Correspondingly, considering the orientation of the bound guests discussed here, esters **4** and **6** would be expected to have the more sterically accessible carboxyl carbon. In short, the unlikely event of hydroxide entering the cavity would lead to the opposite goodness-of-fits observed. Although the precise cause of the small deviations for the fit of esters **2** and **3** remains unclear, the gross model is fairly accurate. The results therefore strongly support the notion that the principle mechanism for hydrolysis of these esters involves guest egress as the rate-limiting step.

Returning to the kinetic resolution of the different esters, it is apparent that the outcome depends on the equilibria between the free and bound species and the relative rate with which the free esters undergo reaction. A high goodness-of-fit with the capsule, coupled with a low reactivity in the free state, will favour a compound remaining unreacted, whereas a poor goodness-of-fit and high reactivity will do the opposite. In this regard, the resolutions described here are analogous to Curtin–Hammett/Winstein–Holness kinetics[37], although there are obviously additional feedback mechanisms in these resolutions (liberated host) that complicate the analysis somewhat. On a different level, there are also complications arising from our choice of system to analyse. The use of Arrhenius plots to estimate reaction rates at 100 °C, and the use of relative binding constants obtained at room temperature (rather than 100 °C) relies on many assumptions, not least of which is that there are no temperature effects on the change in free energy for the binding of each guest. These factors may indeed explain why not all fits shown in Fig. 4 were excellent. That said, this proof-of-principle does suggest future opportunities. For example, the resolution is most certainly controlled in large part by the stoichiometry of the host and guests. In the present case, a sub-stoichiometric amount of host (1:2 ratio of capsule:ester mixture) was used to bias resolution when the difference between the K_{rel} values for the two guests was very large; that is, at the start of the resolution the vast majority of the free ester was the weaker binder. What happens to the resolution with increased or decreased equivalents of host? Can sub-stoichiometric amounts of host (relative to a target compound) still lead to good resolutions? Temperature is also likely an important factor in these processes. Because the reaction of encapsulated ester is very slow at room temperature, intuitively, resolutions involving a large ΔK_{rel} value would be improved at lower temperature. We will study these and other factors in due course. In the mean time, although these types of resolutions are highly dependent on the nature of the host, we are enthused by the structural diversity of the hosts in the literature and the potentially wide range of kinetic resolutions that these could promote.

In summary, we have demonstrated that encapsulation within host $\mathbf{1}_2$ can bring about the kinetic resolution of constitutional isomers of long-chain esters. Moreover, our results demonstrate that the quality of resolution correlates with the difference in the binding constants of the two esters; the larger the difference in the binding constants, the better the kinetic resolution. The difference in the binding constants of paired guests is itself based on a combination of two factors. First, at a general level cavity fitting should be optimal. Second, and more specifically, subtle structural differences between constitutional isomers ideally should result in significant changes in non-covalent contacts between host and guest. Our results also demonstrate that there is more to these resolutions than simple differences in K_{rel}, and we are investigating some of these possibilities. We will report on these findings in due course.

Supplementary Material

Refer to Web version on PubMed Central for supplementary material.

NIH-PA Author Manuscript

NIH-PA Author Manuscript

NIH-PA Author Manuscript

Acknowledgments

B.C.G. acknowledges financial support from the National Science Foundation (NSF; CHE-0718461), the National Institutes of Health (NIH; GM074031) and the Post-Katrina Support Fund Initiative (PKSFI, LEQSF(2007-12)-ENH-PKSFI-PRS-04). S.W.R. acknowledges financial support from the NSF (CHE-0611679). The authors also thank G. Raman and A. Sankaranarayanan for calculating the dipole, log *P* and solubility values of esters **2** to **6**.

References

1. Vriezema DM, et al. Self-assembled nanoreactors. Chem Rev 2005;105:1445–1489. [PubMed: 15826017]
2. Leung DH, Bergman RG, Raymond KN. Highly selective supramolecular catalyzed allylic alcohol isomerization. J Am Chem Soc 2007;129:2746–2747. [PubMed: 17302420]
3. Kaanumalle LS, Gibb CLD, Gibb BC, Ramamurthy V. Controlling photochemistry with distinct hydrophobic nano-environments. J Am Chem Soc 2004;126:14366–14367. [PubMed: 15521751]
4. Kaanumalle LS, Gibb CLD, Gibb BC, Ramamurthy V. A hydrophobic nano-capsule controls the photophysics of aromatic molecules by suppressing their favored solution pathways. J Am Chem Soc 2005;127:3674–3675. [PubMed: 15771483]
5. Kaanumalle LS, Gibb CLD, Gibb BC, Ramamurthy V. Photo-Fries reaction in water made selective with a capsule. Org Biomol Chem 2007;5:236–238. [PubMed: 17205166]
6. Natarajan A, et al. Controlling photoreactions with restricted spaces and weak intermolecular forces: remarkable product selectivity during oxidation of olefins by singlet oxygen. J Am Chem Soc 2007;129:4132–4133. [PubMed: 17362015]
7. Gibb CLD, Sundaresan AK, Ramamurthy V, Gibb BC. Templation of the excited-state chemistry of α-(*n*-alkyl) dibenzyl ketones: how guest packing with a nanoscale supramolecular capsule influences photochemistry. J Am Chem Soc 2008;130:4069–4080. [PubMed: 18321108]
8. Sundaresan AK, Gibb CLD, Gibb BC, Ramamurthy V. Chiral photochemistry in a confined space: torquoselective photoelectrocyclization of pyridones within an achiral hydrophobic capsule. Tetrahedron 2009;65:7277–7288.
9. Sundaresan AK, Kaanumalle LS, Gibb CLD, Gibb BG, Ramamurthy V. Chiral photochemistry within a confined space: diastereoselective photorearrangements of a tropolone and a cyclohexadienone included in a synthetic cavitand. Dalton Trans 2009:4003–4011. [PubMed: 19440600]
10. Pluth MD, Bergman RG, Raymond KN. Acid catalysis in basic solution: a supramolecular host promotes orthoformate hydrolysis. Science 2007;316:85–88. [PubMed: 17412953]
11. Pluth MD, Bergman RG, Raymond KN. Catalytic deprotection of acetals in basic solution with a self-assembled supramolecular 'nanozyme'. Angew Chem Int Ed 2007;46:8587–8589.
12. Pluth MD, Bergman RG, Raymond KN. Supramolecular cataysis of orthoformate hydrolysis in basic solution: an enzyme like mechanism. J Am Chem Soc 2008;130:11423–11429. [PubMed: 18680290]
13. Furusawa T, Kawano M, Fujita M. The confined cavity of a coordination cage suppresses the photocleavage of α-diketones to give cyclization products through kinetically unfavorable pathways. Angew Chem Int Ed 2007;46:5717–5719.
14. Murase T, Sato S, Fujita M. Nanometer-sized shell molecules that confine endohedral polymerizing units. Angew Chem Int Ed 2007;46:1083–1085.
15. Nishioka Y, Yamaguchi T, Kawano M, Fujita M. Asymmetric (2+2) olefin cross photoaddition in a self-assembled host with remote chiral auxiliaries. J Am Chem Soc 2008;130:8160–8161. [PubMed: 18540605]
16. Yamaguchi T, Fujita M. Highly selective photomediated 1,4-radical addition to *o*-quinones controlled by a self-assembled cage. Angew Chem Int Ed 2008;47:2067–2069.
17. Chen J, Körner S, Craig SL, Rudkevich DM, Rebek J Jr. Amplification by compartmentalization. Nature 2002;415:385–386.
18. Hayashida O, Sebo L, Rebek J Jr. Molecular discrimination of *N*-protected amino acid esters by a self-assembled cylindrical capsule: spectroscopic and computational studies. J Org Chem 2002;67:8291–8298. [PubMed: 12444605]

NIH-PA Author Manuscript

NIH-PA Author Manuscript

NIH-PA Author Manuscript

19. Purse BW, Gissot A, Rebek J Jr. A deep-cavitand provides a structured environment for the Menschutkin reaction. J Am Chem Soc 2005;127:11222–11223. [PubMed: 16089433]
20. Iwasawa T, Wash P, Gibson C, Rebek J Jr. Reaction of an introverted carboxylic acid with carbodiimide. Tetrahedron 2007;63:6506–6511. [PubMed: 18612332]
21. Shenoy SR, Crisostomo FRP, Iwasawa T, Rebek J Jr. Organocatalysis in a synthetic receptor with and inwardly directed carboxylic acid. J Am Chem Soc 2008;130:5658–5659. [PubMed: 18393498]
22. Crisostomo FRP, Lkedo A, Shenoy SR, Iwasawa T, Rebek J Jr. Recognition and organocatalysis with a synthetic cavitand receptor. J Am Chem Soc 2009;131:7402–7410. [PubMed: 19469579]
23. Warmuth R, Yoon J. Recent highlights in hemicarcerand chemistry. Acc Chem Res 2001;34:95–105. [PubMed: 11263868]
24. Yebeutchou RM, Dalcanale E. Highly selective monomethylation of primary amines through host–guest product sequestration. J Am Chem Soc 2009;131:2452–2453. [PubMed: 19199632]
25. Vedejs E, Jure M. Efficiency in nonenzymatic kinetic resolution. Angew Chem Int Ed 2005;44:3974–4001.
26. Williams, JMJ.; Parker, RJ.; Neri, C. Enzyme Catalysis in Organic Synthesis. Drauz, K.; Waldmann, H., editors. Wiley-VCH; 2002.
27. Pellissier H. Recent developments in dynamic kinetic resolution. Tetrahedron 2008;64:1563–1601.
28. Martín-Matute B, Bäckvall J. Dynamic kinetic resolution catalyzed by enzymes and metals. Curr Opin Chem Biol 2007:226–232. [PubMed: 17349815]
29. Gibb, BC. Organic Nano-Structures. Atwood, JL.; Steed, JW., editors. John Wiley & Sons; 2007.
30. Liu S, Gibb BC. High-definition self-assemblies driven by the hydrophobic effect: synthesis and properties of a supramolecular nanocapsule. Chem Commun 2008:3709–3716.
31. Ewell J, Gibb BC, Rick SW. Water inside a hydrophobic cavitand molecule. J Phys Chem B 2008;112:10272–10279. [PubMed: 18661937]
32. Gibb CLD, Gibb BC. Templated assembly of water-soluble nano-capsules: inter-phase sequestration, storage and separation of hydrocarbon gases. J Am Chem Soc 2006;128:16498–16499. [PubMed: 17177388]
33. Gibb CLD, Gibb BC. Well defined, organic nano-environments in water: the hydrophobic effect drives a capsular assembly. J Am Chem Soc 2004;126:11408–11409. [PubMed: 15366865]
34. Gibb CLD, Gibb BC. Guests of differing polarities provide insight into structural requirements for templates of water-soluble nano-capsules. Tetrahedron 2009;65:7240–7248. [PubMed: 20606762]
35. Gibb CLD, Gibb B. Straight-chain alkanes template the assembly of water-soluble nano-capsules. Chem Commun 2007:1635–1637.
36. Trembleau L, Rebek J Jr. Helical conformation of alkanes in a hydrophobic cavitand. Science 2003;301:1219–1220. [PubMed: 12947192]
37. Seeman JI. Effects of conformational change on reactivity in organic chemistry. evaluations, applications and extensions of Curtin–Hammett/Winstein–Holness kinetics\. Chem Rev 1983;83:83–134.

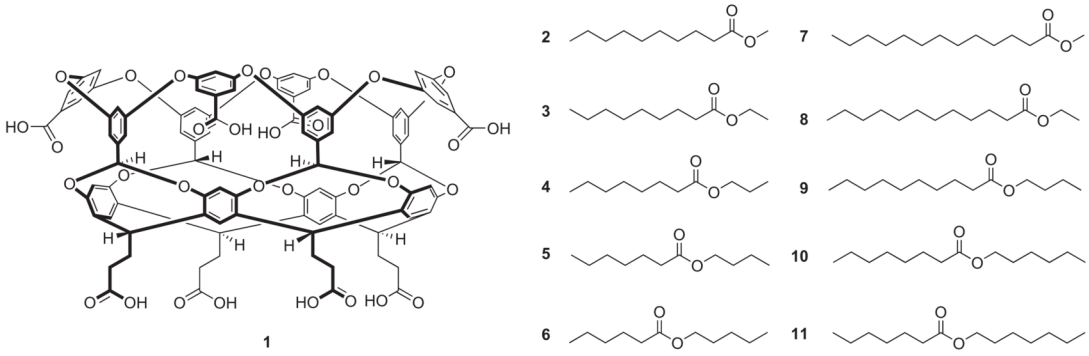

Figure 1. Molecular structures of the host and guests used in this study

Deep-cavity cavitand host **1**, and the two series of ester guests **2–6** (13 non-hydrogen atoms) and **7**–**11** (16 non-hydrogen atoms).

NIH-PA Author Manuscript
NIH-PA Author Manuscript
NIH-PA Author Manuscript

NIH-PA Author Manuscript

NIH-PA Author Manuscript

NIH-PA Author Manuscript

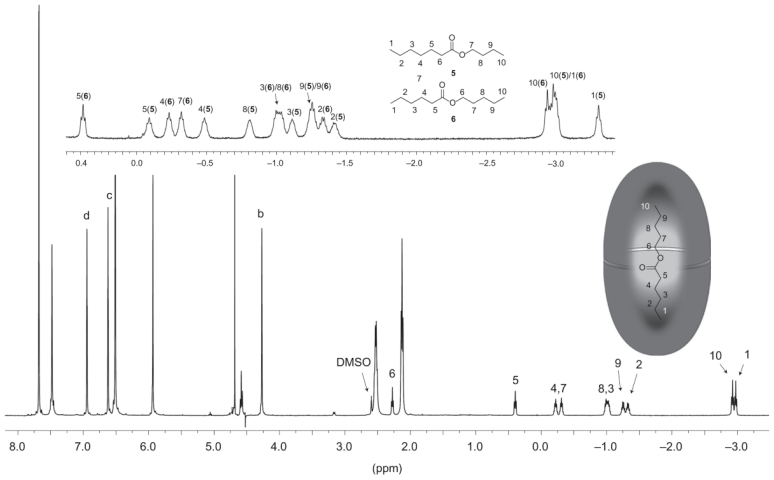

Figure 2. Binding of esters inside a deep-cavity cavitand

Main spectrum: ^{1}H NMR spectrum in D_2O of the 2:1 complex (~1 mM) formed between host **1** and ester **6**. High-field guest signals are highlighted. The residual signal from DMSO-d_6 arises from the necessity to dissolve the ester in a small volume of DMSO-d_6. Upper spectrum: ^{1}H NMR guest binding region for a 2:1:1 ratio of host **1** and esters **5** and **6** (~1 mM host). Integration of selected bound guest signals gives a 0.8:1 ratio of complexes $\mathbf{1}_2$.**5** and $\mathbf{1}_2$.**6**, respectively and allows calculation of the relative binding affinities of each guest.

NIH-PA Author Manuscript

NIH-PA Author Manuscript

NIH-PA Author Manuscript

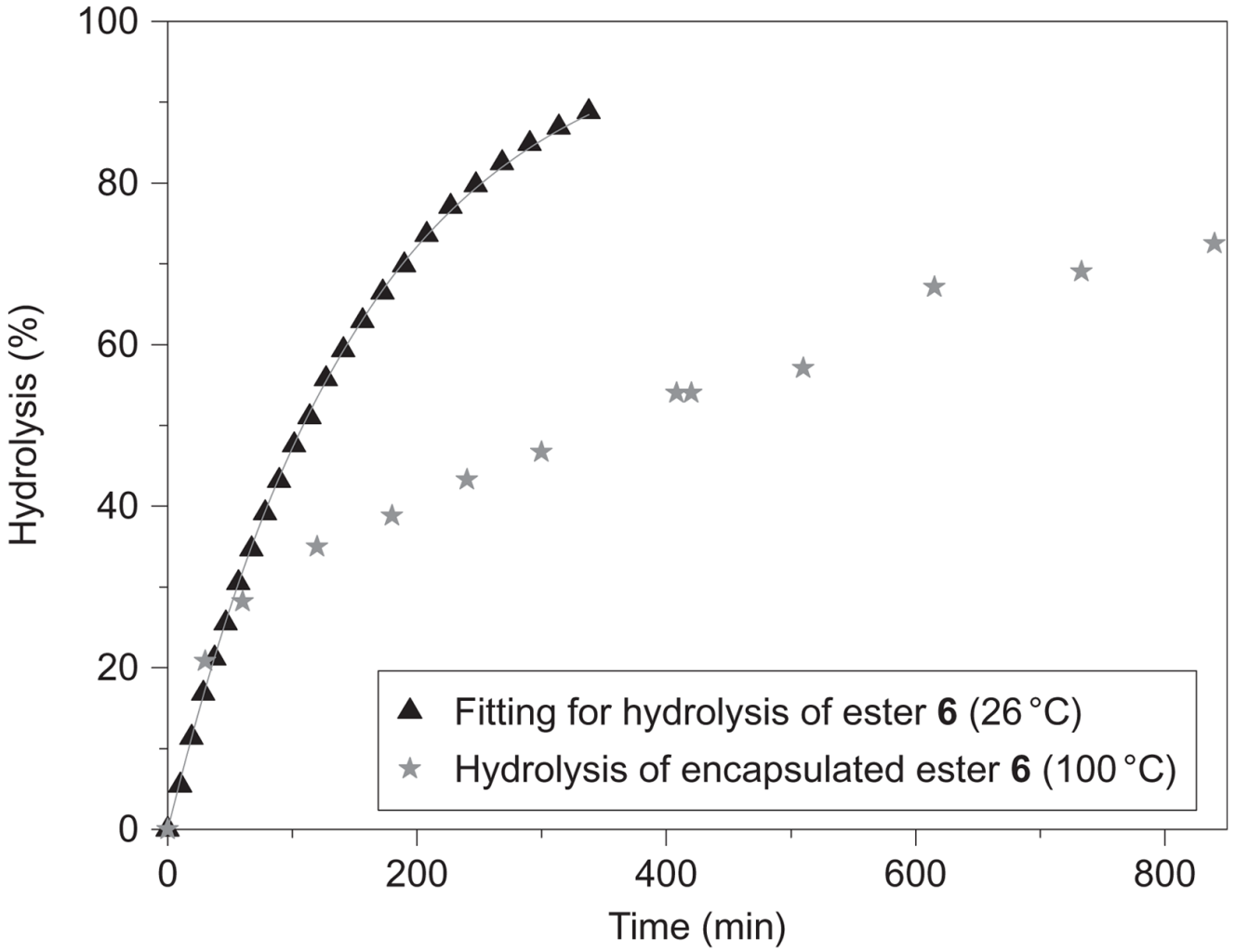

Figure 3. Kinetics for the hydrolysis of ester 6 in the presence or absence of the cavitand

Triangles show the hydrolysis in 3:7 acetone-d_6:D_2O containing 10 mM $NaOH_{aq}$ and ester **6** (0.5 mM) at 26 °C. Stars show the rate of hydrolysis in the presence of capsule $\mathbf{1}_2$ (0.5 mM) at 100 °C in 18 mM $NaOH_{aq}$ (note that 8 equiv. of base are required to deprotonate the capsule). The rate of hydrolysis is slower even at a significantly higher temperature, because the capsule can protect the ester from the hydrolytic environment.

NIH-PA Author Manuscript

NIH-PA Author Manuscript

NIH-PA Author Manuscript

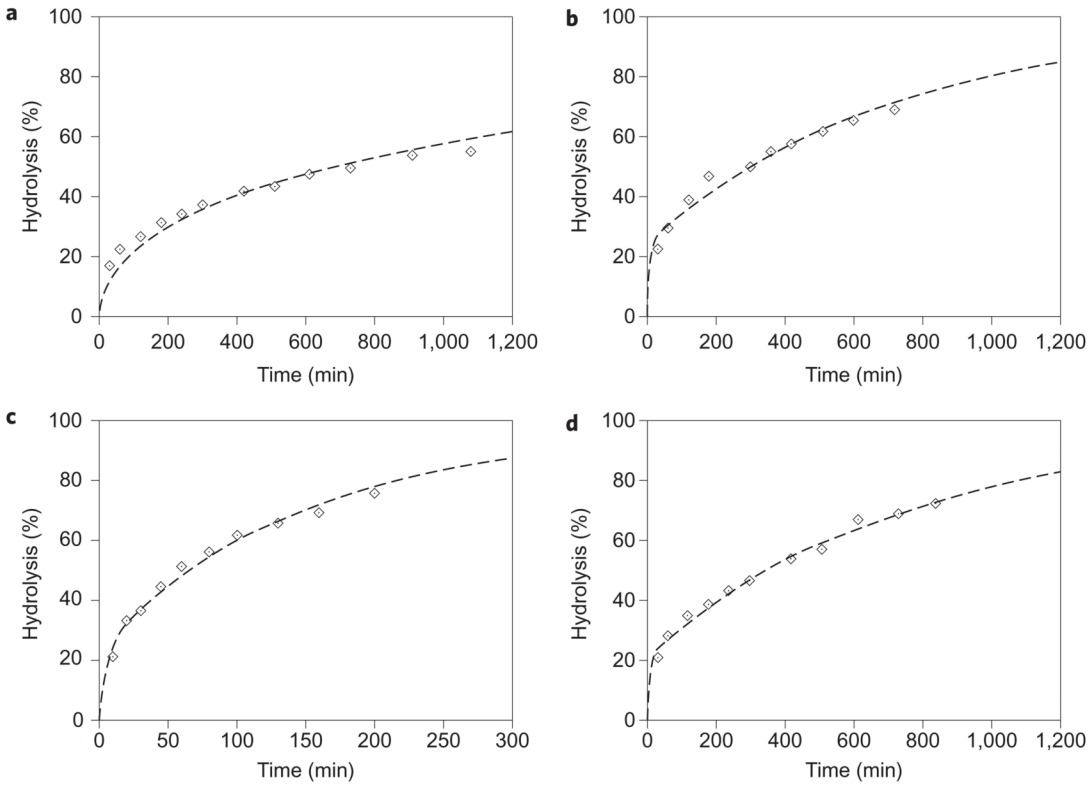

Figure 4. Hydrolysis of similarly sized esters encapsulated within host 1_2

a–d, Observed data are shown as points, and calculated fit curves are shown as dashed lines for the hydrolysis of methyl decanoate (**2**) (**a**), ethyl nonanoate (**3**) (**b**), propyl octanoate (**4**) (**c**) and pentyl hexanoate (**6**) (**d**). Ester **4** is hydrolysed at approximately four times the rate of the other guests.

NIH-PA Author Manuscript NIH-PA Author Manuscript NIH-PA Author Manuscript

Table 1

Calculated physical properties, rate constants for hydrolysis and binding affinity (to capsule 1_2) of esters 2–6.

Ester	Dipole, D*	Log P*	Solubility (M)*	$k_{obs(free)}(s^{-1})$†	$K_{rel}^{‡}$
2	2.41	3.68	1.0×10^{-4}	3.96×10^{-4}	165.4
3	2.52	3.76	6.5×10^{-5}	1.63×10^{-4}	1.8
4	2.51	3.76	6.6×10^{-5}	1.23×10^{-4}	1.0
5	2.54	3.76	6.4×10^{-5}	1.06×10^{-4}	10.7
6	2.54	3.77	6.3×10^{-5}	1.06×10^{-4}	16.4

*Dipole moment, log P (for 1-octanol/water) and aqueous solubility (at 26 °C) calculated using QikProp (Schrodinger).

†At 26 °C in 3:7 acetone-d_6:D_2O, 0.8 mM ester, 10 mM NaOH. For curve fitting, all χ^2/degrees of freedom (DoF) values <2.1; all R^2 values >0.998.

‡For binding to capsule $\mathbf{1}_2$ in (deuterated) aqueous 8 mM $NaHCO_3$. Differences between values are significant.

See Supplementary Information for error analysis.

NIH-PA Author Manuscript
NIH-PA Author Manuscript
NIH-PA Author Manuscript

Table 2

Outcome of competition experiments between pairs of esters 2–6.

Ester*	2	3	4	5	6
2	—				
3	82	—			
4	84	<10	—		
5	46	44	52	—	
6	41	48	56	<10	—

* In D_2O. Concentrations of species: capsule $\mathbf{1}_2$ (0.5 mM), ester ‘a’ (0.5 mM), ester ‘b’ (0.5 mM) and NaOH (18 mM). Numerical values correspond to the percentage remaining of the slower reacting ester (coloured accordingly) when all of the more quickly hydrolysing ester had been consumed.

NIH-PA Author Manuscript NIH-PA Author Manuscript NIH-PA Author Manuscript

Table 3

Activation energies, pre-exponential factors, estimated observed rate constant at 100 °C, and the associated errors for the hydrolysis of free esters 2–6.

Ester*	Activation energy, E_a (kJ mol^{-1})	Error in activation energy, E_a (kJ mol^{-1})	Pre-exponential factor, A (s^{-1})	Error in pre-exponential factor, A (s^{-1})	Rate constant at 373.15 K, k_{obs} (×10^3 s^{-1})	Error in rate constant (k) at 373.15 K, k_{obs} (×10^3 s^{-1})
2	43.1	0.8	13,262	4,469	12.2	0.86
3	40.4	0.8	1,810	596	4.03	0.28
4	38.9	0.5	779	167	2.75	0.12
5	37.6	1.0	387	117	2.13	0.13
6	37.7	0.5	407	85	2.13	0.09

* In 3:7 acetone-d_6:D_2O, 0.8 mM ester, 10 mM NaOH. E_a, A and k values were determined using Microsoft Excel. Errors were determined using Excel linear least-squares curve fitting (LINEST).